Modeling the metabolic adaptations of the biomass under rapid growth and starvation conditions in the activated sludge process

B. Lavallée, P. Lessard, and P.A. Vanrolleghem

Abstract: For wastewater treatment, the activated sludge models (ASMs) 1, 2, and 3 of the International Water Association (IWA) are accepted as industrial standard. However, many authors have observed that the kinetic parameters of these models depend on the type of substrate, process configuration, and sludge age. Some publications showed that the kinetic parameters of ASMs could be influenced by regulation of enzyme production. Therefore, an engineer aiming to make some modifications to a specific system is not able to predict the response of the real system after the modifications and choose the right configuration or modifications with the same set of parameters. On the other hand, cybernetic models are proposed for modeling cell growth and focus, among other things, on regulation of enzyme production, that is to say on induction. Thus, the objective of this paper is to present an activated sludge model that mimics the enzymatic induction of active biomass within the framework of ASMs. In the proposed model, process rates are modulated according to the environmental conditions and cell history. The model is fitted on the basis of data found in the literature. All data collected from short and long transient experiments were fitted with the same set of parameters, which was not possible with other models. The proposed model gives a more realistic picture of active biomass and of its specific activity under highly varying process conditions, but further research is required to support the model with experimental data.

Key words: activated sludge models (ASMs), activity, biomass, enzymes, induction, model, parameter, rate, regulation, sludge, transient.

Résumé : Les modèles de boues activées 1, 2 et 3 de l'International Water Association (IWA) sont acceptés comme normes de l'industrie pour le traitement des eaux usées. Toutefois, plusieurs auteurs ont remarqué que les paramètres cinétiques de ces modèles dépendent du type de substrat, de la configuration du procédé et de l'âge des boues. Certains articles ont indiqué que les paramètres cinétiques des modèles de boues activées pourraient être influencés par la régulation de la production d'enzymes. Ainsi, un ingénieur cherchant à modifier un système spécifique ne peut prédire la réponse du système réel une fois les modifications apportées ni choisir la bonne configuration ou les bonnes modifications avec le même ensemble de paramètres. Aussi, des modèles cybernétiques sont proposés pour modéliser la croissance cellulaire et portent, entre autres, sur la régulation de la production d'enzymes, c'est-à-dire sur l'induction. L'objectif du présent article est donc de présenter un modèle de boues activées qui imite l'induction enzymatique de la biomasse active dans le cadre des modèles de boues activées. Dans le modèle proposé, les taux de réaction sont ajustés aux conditions environnementales et à l'historique cellulaire. Le modèle est calé sur les données trouvées dans la littérature. Les données colligées lors d'expériences transitoires à court et à long termes ont toutes été calées avec le même ensemble de paramètres, ce qui n'était pas possible avec les autres modèles. Le modèle proposé offre ainsi un regard plus réaliste de la biomasse active et de son activité spécifique sous des conditions de procédé hautement variables, mais une recherche plus poussée est requise pour soutenir le modèle avec des données expérimentales.

Mots clés : modèles de boues activées, activité, biomasse, enzymes, induction, modèle, paramètre, taux, régulation, boues, transitoire.

[Traduit par la Rédaction]

1. Introduction

During the last decade, many models were used for to describe behaviour of wastewater treatment plants using activated sludge processes (e.g., Henze et al. 2000). In these models, kinetic parameters that depict the activity of biomass in the processes are assumed constant. The representation of active

Received 10 March 2004. Revision accepted 29 November 2004. Published on the NRC Research Press Web site at http://jees.nrc.ca/ on 15 November 2005.

B. Lavallée[1] and P. Lessard. Département de Génie Civil, Faculté des Sciences et de Génie, Université Laval, Québec, QC G1K 7P4, Canada. **P.A. Vanrolleghem.** Department of Applied Mathematics, Biometrics and Process Control, Ghent University, Coupure Links 653, B-9000 Gent, Belgium.

Written discussion of this article is welcomed and will be received by the Editor until 31 March 2006.

[1]Corresponding author (e-mail: Bernard.Lavallee.1@ulaval.ca).

 doi: 10.1139/S04-082

biomass can therefore be regarded as a static picture of its particular metabolic state. Authors of these models stated that these constant kinetic parameters depend on the type of substrate, process configuration, and sludge age (Henze et al. 2000).

However, the cell's metabolism is the result of a large number of biochemical reactions. These reactions are coordinated and regulated by different inhibitors and inducers. Thousands of enzymes exist, and hundreds could be involved in the active metabolism of the cell (Bailey and Ollis 1986). Consequently, cells have a variable level of specific activity. For instance, Grady et al. (1996) showed that the value of the maximum growth rate of a particular sludge is linked to its metabolic state and is dependent, among others, on the dilution rate in a chemostat. Many authors also showed that the maximum growth rate value will change with the applied substrate to biomass ratio S_0/X_0 in batch experiments (Chudoba et al. 1992; Daigger and Grady 1982*a*; Sin 2004). Furthermore, it was also shown that evaluation of kinetic parameters could be influenced by enzymatic induction (a mechanism inducing the production of a specific enzyme) (Çinar and Grady 2001; Grady et al. 1996; Lavallée et al. 2002; Sin 2004; Vanrolleghem et al. 1998).

Thus, variation in operating conditions of a treatment plant, or modifications made on the system, will induce variation in the specific activity of cells, but the model (with its constant parameters) will give a deviation from the response of the real system. For instance, it is well known that $\mu_{H\,max}$, the maximum growth rate of heterotrophic biomass, will change according to culture conditions (Daigger and Grady 1982*a*). Also, K_{STO}, a parameter of the storage process in ASM3, is not universal, and its value changes with environmental conditions (Hanada et al. 2001). Variation of the process configuration or the operation mode changes the induction time of particular enzymatic chains. Thus, this changes the specific activity level of the biomass and the dependant parameters. A detailed literature review on process induction is given in a separate paper (Lavallée et al. 2005). Therefore, an engineer aiming to optimize the configuration of a system or to modify a specific system is not able to predict the response of the real system after the modifications and choose the right configuration or modifications. Hence, further refinement of current models is desirable for process design and retrofitting.

To model enzymatic induction and metabolic adaptation, biochemical models have already been proposed in the literature (Jensen and Pedersen 1990; Zhang et al. 2002). In these models, the protein synthesis system (PSS) will grow and decay with substrate availability or starvation. The state of the PSS will set the rate of protein formation and thus the growth rate of bacteria (Jensen and Pedersen 1990; Zhang et al. 2002).

Ramkrishna and co-workers (Baloo and Ramkrishna 1991; Kompala et al. 1986; Turner et al. 1989) proposed cybernetic models to mimic enzymatic induction of fast-growing bacteria. In these models, a structured representation of cells is adopted to mimic the growth and decay of some PSS components, called resource machinery. The cybernetic approach is based on an invariant strategy rather than an invariant kinetic response, which is implicit in the framework of kinetic models (Ramkrishna 1983). Mathematical functions are used to model some induction mechanisms in addition to the usual kinetic functions. In these models, the enzymatic pool and resource machinery fluctuate with substrate availability and the history of the microorganisms. These models fit quite well to data collected in chemostat cultures with step variations of dilution rate. Liu et al. (1998) used a cybernetic model to describe the diauxic behaviour of activated sludge in the denitrification process. The significance of this short transient and influence of the induction time (the unaerated volume fraction) in the denitrification process was shown by Lee et al. (2004) using the model proposed by Liu et al. (1998). However, in this cybernetic model, only one component having a short time constant is used to mimic the PSS. Modeling longer transients as growth rate fluctuations (Frigon et al. 2002*a*) requires an additional component having a larger time constant (to mimic the stable RNA). To this end, different metabolic states of cells (that is to say, the adaptation speed of the cells to new conditions (Daigger and Grady 1982*b*)) will be described using these two components (for a review, see Lavallée et al. (2005)). Obviously, the real cellular processes are much more complex than the chosen representation, and several steps and components are not included in the model.

Thus, the objective of this paper is to present a model that mimics the variation of the specific activity of active biomass within the frame of the ASM models. The modifications done to ASM3 aim to model the variation of the process rates (defined in ASM3) and increase the prediction capabilities for a variety of process configurations. With a model able to mimic the regulation of the growth rate, it should be possible to access the intrinsic value of parameters defining the growth rate of biomass. As a consequence, it would be possible to predict the response of continuous systems or semi-continuous systems and batch processes with the same set of parameters. Hence, recalibration of the model to each process configuration would not be required as for ASMs. This will minimise the experimental work. Thus, after the model is calibrated with an effluent data set, it is conceivable that this mathematical tool can be used to perform design optimisation or plant retrofit.

In the proposed model, the biomass description is limited to heterotrophic biomass exposed to aerobic conditions. Extension of the model to anoxic conditions or inclusion of nitrifying biomass and phosphate accumulating organisms will need additional components and processes descriptions. This will be topics of future work.

2. The chosen picture of biomass

It is difficult to choose the representation of biomass when one is building a model. Here, the aim of the proposed model is to describe the varying growth rates of the active cells. The only parameter that does not vary with growth rate is the mass of the cell nucleus. Obviously, growing cells could have more than one copy of the nucleus, but the mass of the nucleus could be

Fig. 1. Diagram of the structured biomass.

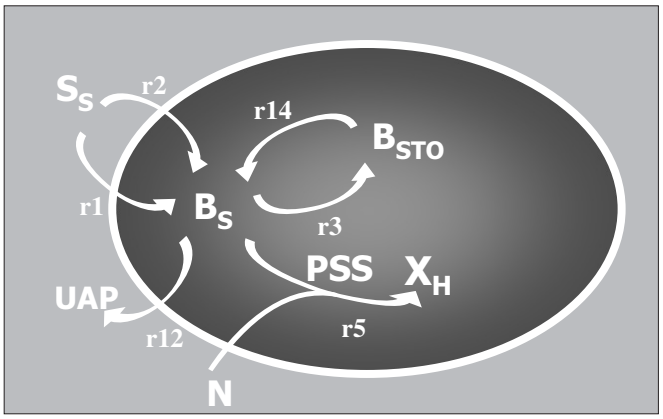

Fig. 2. Details of the PSS.

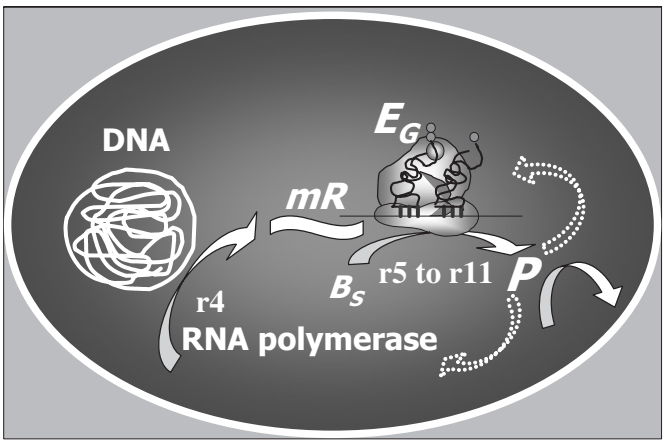

used as a reference (Bremer and Dennis 1996). According to the data presented by Bremer and Dennis (1996) for *Escherichia coli* and Daigger and Grady (1982*b*) for *Pseudomonas putida*, the ratio of structural proteins (total proteins minus ribosomal proteins) to DNA remains constant for all growth rates. Also, Schaechter et al. (1958) suggested that the ratio of cell wall and membrane per nucleus remains constant for all growth rates. Their hypothesis is based on their observations that the ratio "surface areas of cell wall/nucleus" remains virtually constant. The same assumption is taken in the proposed model, and the cells will be represented by X_H, the mass of structural components built of one nucleus, and the corresponding amount of cell membrane and cell wall. Because the ratio of these structural components is assumed to be constant, the evaluation of active cells should be performed by measurement of the DNA concentration. Obviously, the model will not describe the various growth rates of a distributed population of bacteria, and it will model the mean growth rate of all cells.

Different components are use to structure the chosen representation of biomass. The biomass chemical oxygen demand (COD) consists of endogenous substrate, endogenous reserves as glycogen or PHA, a simplified representation of the PSS, and a structural component. Specific model components are used to describe particular enzymes and their associated rates. The enzymes produce the metabolites used by the cell for growth and are those describing the reactions shown in Fig. 1. A similar representation was initially proposed by Dircks et al. (2001) and was adapted by Lavallée et al. (2005). In Fig. 1, substrate (S_S) is taken up by the cell to form an endogenous substrate (B_S). The cell can grow on this endogenous substrate, make stored products (B_{STO}), or produce utilization-associated products (UAP). The numbers (r*X*) close to the arrows in Fig. 1 are the process numbers corresponding to the Peterson matrix (Table 1).

Proteins make up the main part of cell mass (Bremer and Dennis 1996; Daigger and Grady 1982*a*; Herbert 1976). Thus, exponential growth could be seen as an increase in proteins (Zhang et al. 2002). This implies that growth and growth regulation are coupled to the state of the PSS, which sets the rate of protein formation (Zhang et al. 2002). In short, three components, i.e., messenger RNA (mRNA), ribosome (or rRNA), and RNA polymerase, make up the PSS. Proteins are synthesized in two steps. During the first step, the transcription step, the RNA polymerase transcribes the DNA code to produce mRNA. In the second step, the translation step, ribosomes translate the mRNA to produce proteins. During exponential growth, the number of ribosomes (the part of the PSS that assembles the proteins) shows a linear relationship with the growth rate of the cells (Bremer and Dennis 1996). Therefore, in the proposed model, the metabolic state of the active biomass is introduced via a simplified representation of the PSS (Lavallée et al. 2005). The PSS representation is given in Fig. 2. Transcription and translation are two key steps in protein synthesis (Zhang et al. 2002). The RNA polymerase limits the rate of transcription, i.e., synthesis of mRNA (Zhang et al. 2002), and its expression is regulated proportionally to the amount of ribosome proteins (Berlyn et al. 1996). Messenger RNA (mRNA) has a short half-life, while rRNA, which constituted a fixed fraction of the ribosomes, has a longer half-life. Thus, in the model it is assumed that mRNA is modeled by the short half-life component of the PSS, mR, and stable rRNA is modeled by the growth enzyme, E_G. Because RNA polymerase is coexpressed with ribosome proteins, it is modeled with the variable E_G, too. Hence, in the model, mRNA is produced by E_G (RNA polymerase), and the latter is required as ribosomes for protein (P) or enzyme production.

The modeled processes are descriptions of the real processes. Therefore, the values of parameters should be chosen within the range of the values found in the literature with respect to time constants.

3. The proposed model

In the following paragraphs, the processes in Figs. 1 and 2 are presented in a mathematical formulation. A complete mathematical description of the model is given in Tables 1–3, using the Peterson matrix notation. In the proposed model, the notation X refers to suspended material, and S refers to soluble material, as in ASM models. The notation B refers to endogenous material, as building blocks, and E refers to an enzymatic structure. The concentrations of these are expressed as *X*, *S*, *B*,

Table 1. Processes description.

Rates	Description	Processes
$R1$	Production of B_S	$k^{max}_{B_{S(1)}} \frac{E_{B_{S(1)}}}{X_H} \frac{S_S}{K_{S(1)}+S_S} \frac{S_O}{K_O+S_O} X_H$
$R2$	Production of B_S	$k^{max}_{B_{S(2)}} \frac{E_{B_{S(2)}}}{X_H} \frac{S_S}{K_{S(2)}+S_S} \frac{S_O}{K_O+S_O} X_H$
$r3$	Production of B_{STO}	$k^{max}_{STO} \frac{E_{STO}}{X_H} \frac{B_S/X_H}{K_{B_S}+B_S/X_H} X_H$
$r4$	Production of mR	$\alpha_{mR} \frac{E_G}{X_H} \frac{B_S/X_H}{K_{B_S}+B_S/X_H} \frac{S_O}{K_O+S_O} \frac{S_{NH}}{K_{NH}+S_{NH}} X_H$
$r5$	Growth of heterotrophs and production of E_G	$\mu^{int}_{H\,max} \frac{E_G}{X_H} \frac{[mR]/X_H}{K_{mR}+[mR]/X_H} \frac{B_S/X_H}{K_{B_S}+B_S/X_H} \frac{S_O}{K_O+S_O} \frac{S_{NH}}{K_{NH}+S_{NH}} X_H$
$r6$	Production of E_{STO}	$\alpha_{E_{STO}} \frac{E_G}{X_H} \frac{[mR]/X_H}{K_{mR}+[mR]/X_H} \frac{B_S/X_H}{K_{B_S}+B_S/X_H} \frac{S_O}{K_O+S_O} \frac{S_{NH}}{K_{NH}+S_{NH}} X_H$
$r7$	Production of $E_{B_{S(1)}}$	$\alpha_{E_{BS(1)}} \frac{E_G}{X_H} \frac{[mR]/X_H}{K_{mR}+[mR]/X_H} \frac{S_S}{K_{S(1)}+S_S} \frac{B_S/X_H}{K_{B_S}+B_S/X_H} \frac{S_O}{K_O+S_O} \frac{S_{NH}}{K_{NH}+S_{NH}} \frac{K_{S(2)}}{K_{S(2)}+S_S} X_H$
$r8$	Production of $E_{B_{S(2)}}$	$\alpha_{E_{BS(2)}} \frac{E_G}{X_H} \frac{[mR]/X_H}{K_{mR}+[mR]/X_H} \frac{S_S}{K_{S(2)}+S_S} \frac{B_S/X_H}{K_{B_S}+B_S/X_H} \frac{S_O}{K_O+S_O} \frac{S_{NH}}{K_{NH}+S_{NH}} X_H$
$r9$	Production of E_A	$\alpha_{E_A} \frac{E_G}{X_H} \frac{[mR]/X_H}{K_{mR}+[mR]/X_H} \frac{B_S/X_H}{K_{B_S}+B_S/X_H} \frac{S_O}{K_O+S_O} \frac{S_{NH}}{K_{NH}+S_{NH}} X_H$
$r10$	Production of E_T	$\alpha_{E_T} \frac{E_G}{X_H} \frac{[mR]/X_H}{K_{mR}+[mR]/X_H} \frac{B_S/X_H}{K_{B_S}+B_S/X_H} \frac{S_O}{K_O+S_O} \frac{S_{NH}}{K_{NH}+S_{NH}} X_H$
$i11$	Production of E_h	$\alpha_{E_h} \frac{E_G}{X_H} \frac{[mR]/X_H}{K_{mR}+[mR]/X_H} \frac{X_S}{K_{X_S}+X_S} \frac{K_{S(1)}}{K_{S(1)}+S_S} \frac{B_S/X_H}{K_{B_S}+B_S/X_H} \frac{S_O}{K_O+S_O} \frac{S_{NH}}{K_{NH}+S_{NH}} X_H$
$r12$	Release of B_S	$k^{max}_{RB_S} \frac{B_S/X_H}{K_{RB_S}+B_S/X_H} X_H$
$r13$	Hydrolysis	$k^{max}_h \frac{X_S}{K_{X_S}+X_S} E_h$
$r14$	Degradation of B_{STO}	$\delta k^{max}_{STO} \frac{E_{STO}}{X_H} \frac{B_{STO}/X_H}{K_{STO}+B_{STO}/X_H} \frac{K_{S(1)}}{K_{S(1)}+S_S} X_H$
$r15$	Decay of E_G	$\beta_{E_G} E_G$
$r16$	Decay of E_{STO}	$\beta_{E_{STO}} E_{STO}$
$r17$	Decay of $E_{B_{S(1)}}$	$\beta_{E_{BS}} E_{B_{S(1)}}$
$r18$	Decay of $E_{B_{S(2)}}$	$\beta_{E_{BS}} E_{B_{S(2)}}$
$r19$	Decay of mR	$\beta_{mR}[mR]$
$r20$	Decay of E_A	$\beta_{E_A} E_A$
$r21$	Decay of E_T	$\beta_{E_T} E_T$
$r22$	Decay of E_h	$\beta_{E_h} E_h$
$r23$	Death of biomass cause by toxin	$b^{max}_{X_T} \frac{E_T}{X_H} \frac{K_{iT}}{K_{iT}+E_A/X_H} X_H$
$r24$	Aerobic growth of protozoa	$\mu_{MF\,max} \frac{X_H/X_{MF}}{K_{X/MF}+X_H/X_{MF}} \frac{S_O}{K_{MFO}+S_O} X_{MF}$
$r25$	Decay of protozoa	$b_{MF} X_{MF}$

and E, respectively, and are given in milligrams per litre. When the enzymatic component is expressed in a specific value, the notation is expressed as E/X_H. The variable mR is used to mimic some components of the PSS, such as mRNA, and is equivalent to an enzymatic structure. In the text, rX refer to the processes rate in Table 1. Also, in the text saturation term using O_2 and NH_4 are omitted from most of the equations. However, when required these terms are included in the equations of Table 1.

3.1. Modeling the growth rate fluctuations

In the proposed model, growth of heterotrophic organisms is regulated by concentrations of mR, E_G, and B_S. The concentration of ribosomes (rRNA) is mimicked by the variable E_G. So, the relative concentration of ribosomes within the cell is given by the ratio E_G/X_H.

As shown in eq. [1], the ratio E_G/X_H is added to the growth rate equation proposed by Monod (1949). The ratio E_G/X_H reflects the metabolic state of the active biomass. It will change the growth rate of heterotrophic organisms, μ_H, according to the ribosomes concentration and to RNA theory (Lavallée et al. 2005). As mRNA (mR) is required for the maximal rate of translation by ribosomes, a Michaelis–Menten equation is inserted in the proposed equation, too (Lavallée et al. 2005). The saturation equation including mR will change the μ_H value according to the availability of mRNA (Lavallée et al. 2005; Roels 1982; Vanrolleghem et al. 1998). This term will mimic the specific translation rate of ribosome. B_S is the representation of the endogenous substrate or metabolites and building blocks.

$$[1] \qquad \mu_H = \mu^{int}_{H\,max} \frac{E_G}{X_H} \frac{[mR]/X_H}{K_{mR}+[mR]/X_H} \frac{B_S/X_H}{K_{B_S}+B_S/X_H}$$

The production rate of E_G (process r5 in Table 1) is described by eq. [2] when O_2 and NH_4 are at saturation level. As shown in Fig. 1, it is assumed that the ribosome (E_G) production is

Table 2. Stoichiometry of intracellular, soluble and particulated components.

Rate	E_G (COD, g/m^3)	B_{STO} (COD, g/m^3)	B_S (COD, g/m^3)	S_S (COD, g)	S_O (COD, g)	S_{NH} (N, g)	X_H (COD, g)	X_{MF} (COD, g)	X_i (COD, g)	X_S (COD, g)
$r1$			Y_{BS}	-1	$-(1-Y_{BS})$					
$r2$			Y_{BS}	-1	$-(1-Y_{BS})$					
$r3$		1	-1							
$r4$										
$r5$	φ_{EG}		$\frac{-(1+\varphi_{E_G})}{Y_H}$		$\frac{-(1+\varphi_{E_G})(1-Y_H)}{Y_H}$	$-(1+\varphi_{E_G})i_{XB}$	1			
$r6$										
$r7$										
$r8$										
$r9$										
$r10$										
$i11$										
$r12$			-1	1						
$r13$				1		i_{XB}				-1
$r14$		-1	1							
$r15$	$-(1-Y_H)$				$-(1-Y_H)$	$i_{XB}(1-Y_H)$				
$r16$										
$r17$										
$r18$										
$r19$										
$r20$										
$r21$										
$r22$										
$r23$	$-\frac{E_G}{X_H}$	$-\frac{B_{STO}}{X_H}$	$-\frac{B_S}{X_H}$	$\frac{B_S+B_{STO}}{X_H}$			-1		$\frac{f_u(X_H+E_G)}{X_H}$	$\frac{(1-f_u)(X_H+E_G)}{X_H}$
$r24$	$-\frac{E_G}{X_H Y_{MF}}$	$-\frac{B_{STO}}{X_H Y_{MF}}$	$-\frac{B_S}{X_H Y_{MF}}$	i	$\frac{-(1-Y_{MF})(X_H+E_G+B_S+B_{STO})}{Y_{MF} X_H}$	$\frac{(1-Y_{MF})(X_H+E_G)i_{XB}}{Y_{MF} X_H}$	$-\frac{1}{Y_{MF}}$	$\frac{(1-f_u)(X_H+E_G+B_S+B_{STO})}{X_H}$	$\frac{f_u(X_H+E_G+B_S+B_{STO})}{X_H}$	
$r25$								-1		1

Table 3. Stoichiometry of enzymatic components.

Rate	E_{STO} (unit/L)	$E_{BS(1)}$ (unit/L)	$E_{BS(2)}$ (unit/L)	[mR] (unit/L)	E_A (unit/L)	E_T (unit/L)	E_h (unit/L)
$r1$							
$r2$							
$r3$							
$r4$				1			
$r5$							
$r6$	1						
$r7$		1					
$r8$			1				
$r9$					1		
$r10$						1	
$i11$							1
$r12$							
$r13$							
$r14$							
$r15$							
$r16$	-1						
$r17$		-1					
$r18$			-1				
$r19$				-1			
$r20$					-1		
$r21$						-1	
$r22$							-1
$r23$	$-\frac{E_{STO}}{X_H}$	$-\frac{E_{BS(1)}}{X_H}$	$-\frac{E_{BS(2)}}{X_H}$	$-\frac{[mR]}{X_H}$	$-\frac{E_A}{X_H}$	$-\frac{E_T}{X_H}$	
$r24$	$-\frac{E_{STO}}{X_H Y_{MF}}$	$-\frac{E_{BS(1)}}{X_H Y_{MF}}$	$-\frac{E_{BS(2)}}{X_H Y_{MF}}$	$-\frac{[mR]}{X_H Y_{MF}}$	$-\frac{E_A}{X_H Y_{MF}}$	$-\frac{E_T}{X_H Y_{MF}}$	
$r25$							

dependent on the rate of translation (Lavallée et al. 2005), or in other words, of the E_G/X_H and $[mR]/X_H$ levels. Accordingly the E_G/X_H ratio and saturation equation for [mR] are introduced in eq. [2]. The parameter φ_{E_G} is a stoechiometric coefficient related to the correlation between the growth rate and the protein production. The dependency on the availability of amino acids is mimicked by including the endogenous substrate B_S term.

$$[2] \qquad r5_{(E_G)} = \varphi_{E_G} \mu^{int}_{H\,max} \frac{E_G}{X_H} \frac{[mR]/X_H}{K_{mR} + [mR]/X_H} \times \frac{B_S/X_H}{K_{B_S} + B_S/X_H} X_H$$

$$[3] \qquad r4 = \alpha_{mR} \frac{E_G}{X_H} \frac{B_S/X_H}{K_{B_S} + B_S/X_H} X_H$$

In eq. [3] the α_{mR} parameter is the maximal production rate of the mR components. The expression of mR (or its rate of production $r4$) is completely inductive, and changes with the B_S and E_G concentrations. The RNA polymerase concentration is represented in eq. [3] by the ratio E_G/X_H. The number of RNA polymerases per nucleus is proportional to the amount of ribosome, and this for all growth rates (Bremer and Dennis 1996). Thus, the specific RNA polymerase concentration will be mimicked by the variable E_G and the ratio E_G/X_H. The activity of the RNA polymerases is different to the ribosome activity and is therefore modeled by the rate α_{mR}.

In the model, the variable E_G has COD units. Hence, the active biomass COD is now composed of an amount of structural component (X_H) and a variable fraction, the biosynthetic constituent (E_G). The constituent E_G is endogenous; thus the mathematical description of biomass becomes $(X_H + E_G)$. This description agrees with the description of biomass proposed by Masson et al. (1986) and van den Berg (1998). Thus, in the model, the specific COD of active biomass (COD/X_H) will rise and fall with E_G.

The decay of E_G (process r15) and mR (process r19) are endogenous processes described as first-order reactions characterized by the "endogenous" rate constants β_{E_G} and β_{mR}. This formulation is similar to the one used by Baloo and Ramkrishna (1991) for the decay of endogenous enzymes.

3.2. Modeling the substrate uptake rate

It was observed by several authors that the specific substrate uptake rate varies with growth conditions (Ferenci 1999; Kovárová-Kovar and Egli 1998). It was also observed that the rate of substrate uptake and storage in ASM3, is not universal, and the value of this constant changes with environmental conditions (Hanada et al. 2001). It was furthermore shown that the substrate uptake rate is dependent on the concentration of

several transport enzymes in the cell wall (Ferenci 1999).

In the model, readily biodegradable organic substrate (S_S) is taken up by the transport enzyme (E_{B_S}) to yield endogenous substrate (B_S). The accumulation rate is regulated by enzyme and substrate concentration. In this process, the variation of the specific substrate uptake rate will be mimicked by the ratio E_{B_S}/X_H in eq. [4] (processes r1 and r2 in Table 1). Modeling of the production of transport enzymes will be done with an equation similar to the one proposed for production of E_G. The constant $k_{B_S}^{max}$ is the maximum specific activity of the enzyme.

$$[4] \quad r1 \text{ or } r2 = k_{B_S}^{max} \frac{E_{B_S} 1 \text{ or } 2}{X_H} \frac{S_S}{K_{S(1 \text{ or } 2)} + S_S} \frac{S_O}{K_O + S_O} X_H$$

However, the K_S constant could change with substrate, substrate concentration, and growth conditions (Ferenci 1999; Kovárová-Kovar and Egli 1998). Ferenci (1999) showed that the level of expression of various transport enzymes of glucose is regulated by the substrate concentration. At low substrate concentrations, a transport enzyme with a high substrate affinity would be induced at a higher intensity than a second transport system with a low substrate affinity, which is favoured at high glucose concentrations. Thus, the model includes two transport systems (processes r1 and r2) with respective enzymes ($E_{B_{S(1)}}$ and $E_{B_{S(2)}}$) and saturation constants ($K_{S(1)}$ and $K_{S(2)}$). According to Ferenci (1999), in the model, $E_{B_{S(1)}}$ production will be subject to catabolite repression at high substrate concentration.

3.3. Modeling the formation of endogenous reserves

It is well known that in some conditions cells store substrate in the form of glycogen or PHB. Cells able to quickly use and store substrate possess a selective advantage over cells that cannot (van Loosdrecht et al. 1997).

Modeling of storage product formation (process r3) is done as suggested by Dircks et al. (2001) for glycogen and Beun et al. (2000) for PHB. Storage products (B_{STO}) are synthesized from endogenous substrate (B_S) through a single reaction.

$$[5] \quad r3 = \left(k_{STO}^{max} \frac{E_{STO}}{X_H} \frac{B_S/X_H}{K_{B_{S(2)}} + B_S/X_H} \right) X_H$$

Also, as shown on Fig. 1, degradation of storage product is modeled by a single reaction, and this process produces B_S. According to the expression of glycogen enzymes, the enzymes that synthesize and depolymerize B_{STO} are coexpressed by the same operon (Lavallée et al. 2005). Therefore, these two enzymes should be modeled by the variable E_{STO} and the rates k_{STO}^{max} and δk_{STO}^{max}. Obviously, depolymerization of B_{STO} (process 14) is regulated by its concentration and inhibited by high levels of B_S, as shown in eq. [6].

$$[6] \quad r14 = \left(\delta k_{STO}^{max} \frac{E_{STO}}{X_H} \frac{B_{STO}/X_H}{K_{STO} + B_{STO}/X_H} \times \frac{K_{S(1)}}{K_{S(1)} + S_S} \right) X_H$$

Fig. 3. Production rates of soluble microbial products (SMPs).

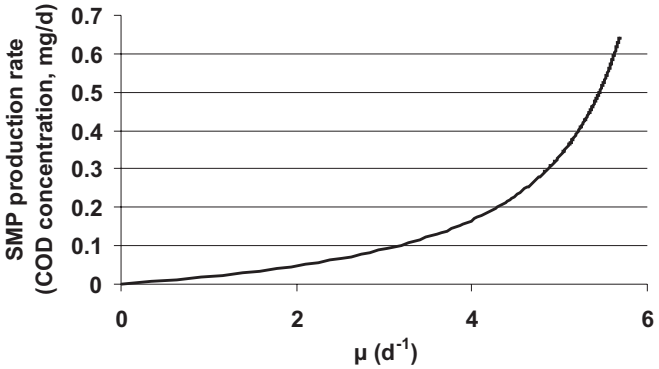

The process rates are modulated by the ratio E_{STO}/X_H. Similar to E_G, production of E_{STO} is regulated at the transcription level. Consequently, the rate of formation or degradation of endogenous reserves will be modulated according to environmental conditions, as observed by Hanada et al. (2001).

3.4. Modeling the formation of soluble microbial products

In addition to the storage process, release of metabolites by the cell is often observed (Grady et al. 1972; Hao and Lau 1988; Huang and Cheng 1987). Utilization-associated product formation may be significant, and the TOC or COD mass balance should take it into account.

Equation [7] models this process (r12).

$$[7] \quad r12 = k_{RB_S}^{max} \frac{B_S/X_H}{k_{RB_S} + B_S/X_H} X_H$$

In this equation, the constant $k_{RB_S}^{max}$ mimics the outward diffusion of metabolites through the cell membrane. A saturation equation is used to model this process. Thus, diffusion of metabolites through the cell membrane will be negligible at low B_S concentrations and proportional to high B_S concentrations. The B_S diffusion will increase according to an exponential function relative to the growth rate. The half-saturation coefficients K_{B_S} used in the growth equation could be set at a lower value than k_{RB_S} used in eq. [7]. Thus, an excess of endogenous substrate will not significantly increase the growth rate, but it will induce an increasing release of B_S in the bulk liquid (Fig. 3). This relation is in accordance with the exponential relation proposed by Hao and Lau (1988) for modeling UAP in a chemostat. Obviously, the real process is more complex than this representation, but for modeling convenience, a single-step formulation is adopted, as was also done for storage formation. Moreover, because nitrogen is required for growth and is not required for UAP formation, this representation presents the opportunity to model the UAP formation under nitrogen-limiting conditions. Also, a balance evaluation of storage on UAP formation is possible because the two processes are in competition for B_S utilization.

The formation of soluble biomass associated products, which are released after exhaustion of the substrate, has not been modeled yet. However, this process has a significant impact on the

COD concentration in the effluent, and it will be included in the model after completion of further modeling studies.

3.5. Modeling the maintenance process

The decay of E_G (β_{E_G}) is a continuous process and thus occurs during both starvation and growth. Therefore, the biomass ($E_G + X_H$) uses substrate to maintain ribosome concentrations at the desired level. The renewal of these enzymes will use the COD, and a part will be used for respiration. This will be assumed to be the maintenance process. Thus, the E_G production and decay are a cycling process quite similar to the maintenance process proposed by Pirt (1965). According to Pirt (1965), maintenance is the use of substrate for other purposes than growth. Thus, in the model, the maintenance is proportional to the macromolecules turnover as proposed by some authors (Chudoba et al. 1992; van den Berg 1998). Then, oxygen used in the energy production process is coupled to the production of enzymes and the growth of active biomass. The decaying macromolecule E_G is used for energy production and leads to endogenous respiration and a loss of specific activity. Thus, the exogenous and endogenous respiration of active biomass are regulated as proposed by some authors (Beeftink et al. 1990; Nicolaï et al. 1991), with the model combining the Herbert (1958) and Pirt (1965) formulations of endogenous and maintenance metabolism, respectively.

Additionally, some energy could be spent in futile cycles as metabolites are released (Hao et Lau 1988). In this process, the constant k_{RBS}^{max} mimics the outward diffusion of metabolites through the cell membrane. Thus, with the combination of the substrate uptake process and the release process, energy is spent in substrate uptake and release cycling.

Several additional processes could be included in the maintenance process (Lavallée et al. 2005), but only some are included in the proposed equations to keep the complexity of the model at a reasonable level.

3.6. Modeling decay and death of active cells

As explained below, the proposed model makes a distinction between endogenous respiration and death of active biomass. The usual concept of active biomass decay includes grazing (process r24) and the influence of other external factors on cells (external decay as proposed by van Loosdrecht and Henze (1999)). Predation is a complex phenomenon that could be modeled with simple processes as in *River Water Quality Model No. 1* (Reichert et al. 2001). However, there is a general lack of information in the literature on kinetic description of grazing by protozoa in activated sludge. Future work will focus on DNA extraction, as done by Brands et al. (1994), and inhibition of protozoa to give some information on the kinetics of cell death.

In the model, microfauna are modeled as a whole. Theyt graze on active bacteria and a cause decrease in the active biomass. Initially, a Lotka–Voltera equation form is adopted for modeling of microfauna growth (process r24). The microfauna component (X_{MF}) is associated with COD used and respiration. Also, the nitrogen fraction is assumed to be the same in microfauna as in active biomass. Therefore, respiration of micro fauna releases nitrogen in proportion to (1 - Y_{MF}). Decay of X_{MF} is modeled by a simple first-order reaction (process r25).

On the other hand, the concept of cell death is proposed here (process r23 in Table 1); it consists of lysis and other internal factors affecting the cell. Death of active biomass can be induced by a toxin–antitoxin couple (TA) (Yarmolinsky 1995). The TA is produced by an inductive process that depends on the substrate concentration in the mixed liquor. The antitoxin (E_A) is produced by the cell during growth at a higher rate than the toxin and neutralize the effect of the toxin (E_T). However, antitoxin has a shorter half-life than the toxin, as shown by Aizenman et al. (1996). Thus, as suggested by Aizenman et al. (1996), only a short time after substrate depletion, the toxin could turn on its bactericidal effect (b_{XT}^{max}) (for a review see Lavallée et al. 2005). E_A and E_T are functional components required for modeling, but not directly identifiable chemically. In the model, the toxin exerts its bactericidal effect when the E_A/X_H ratio is low as described by the Michaelis–Menten term in eq. [9].

The rates of production of the toxin and its antitoxin (processes r10 and r9, respectively) are described as inductive processes dependent on endogenous substrate B_S and of the PSS state. Their decay is a simple first order process with different specific rates to account for the differences in half-life. Modeling of antitoxin (eq. [8]) or toxin production will be done with an equation similar to the one proposed for production of E_G.

$$[8] \qquad r9 = \alpha_{E_A} \frac{E_G}{X_H} \frac{[mR]/X_H}{K_{mR} + [mR]/X_H} \frac{B_S/X_H}{K_{B_S} + B_S/X_H} X_H$$

Modeling of TA action on active biomass (process r23) is done with the following equation for the toxin-induced death:

$$[9] \qquad r23 = b_{X_T}^{max} \frac{E_T}{X_H} \frac{K_{iT}}{K_{iT} + E_A/X_H} X_H$$

In this equation, K_{iT} is the half-saturation coefficient of the toxin-induced death that is inhibited by the presence of the antitoxin.

3.7. Modeling the hydrolysis process

Previously, it was shown that variation of the hydrolysis process could be significant in evaluation of the COD fraction of the influent (Haïder et al. 2000). Here, for the same wastewater, the hydrolysis activities and COD fractions were found to be highly dependent on the sludge activity levels and the food to micro-organisms ratio. On the other hand, Frigon et al. (2002*b*) showed that different populations (the *Acinetobacter* spp., and an actinomycete) within the sludge could use different substrates (as S_S and X_S) for growth. Therefore, a model should mimic the variable ability of sludge to hydrolyse suspended substrate (X_S).

In the model, the hydrolysis rate (process r13) changes according to the specific density of hydrolytic enzymes E_h (eq. [10]). Indeed, hydrolytic enzyme expression is regulated by the substrate or substrate derivatives (Priest 1992). In the model

it is assumed that X_S concentration (thus the derivatives) induces the production of hydrolytic enzymes. On the other hand, hydrolytic enzyme expression is subject to catabolite repression (Priest 1992). Hence, a switching function is added in the hydrolytic enzymes synthesis rate equation to mimic catabolic repression. Thus, enzymes will be produced only when the soluble substrate concentration, and thus the observed growth rate, is low (eq. [11] and process r11). In addition, hydrolytic enzymes will be produced only when the necessary substrate concentrations are high. They are exogenous enzymes and are not affected by growth rate or decay of active biomass.

$$[10] \qquad r13 = k_h^{max} \frac{X_S}{K_{X_S} + X_S} E_h$$

$$[11] \qquad r11 = \alpha_{E_h} \frac{E_G}{X_H} \frac{[mR]/X_H}{K_{mR} + [mR]/X_H} \frac{X_S}{K_{X_S} + X_S} \times \frac{K_{S(1)}}{K_{S(1)} + S_S} \frac{B_S/X_H}{K_{B_S} + B_S/X_H} X_H$$

In eq. [10], the substrate saturation function is adopted because Goel et al. (1998) showed that cellulose hydrolysis is dependent mainly on the enzyme concentration in the mixed liquor. Also these authors showed that hydrolysis process is independent of the electron donor. Finally, E_h/X_H models in the enzyme density per cell or flock surface used in the ASM, as shown in eq. [12].

$$[12] \qquad k_h^{max} E_h = k_h^{max} \frac{E_h}{X_H} X_H$$

The surface saturation function adopted in the ASM should be considered as a specific application of the more general representation chosen here.

4. Estimation of parameters

A number of new parameters are proposed in the model, which includes 17 state variables and 41 parameters. This is seven state variables and 20 parameters more than used in ASM3 for description of heterotrophic biomass in aerobic conditions. Hence, new methods are required for evaluation of state variables and parameter identification. They are proposed in the following paragraphs. These new methods are based on transient behaviour data. These data are usually discarded when using ASMs because it is not possible to fit the responses of the models to these data. Transient behaviour data give additional information compared with the steady state or the usual dynamic data. With these rich information data a multi-steps identification procedure can be used to identify parameters one by one. Each parameter can be identified on a particular transient behaviour according to the transient time constants. Thus, identification of each parameter can be done independently.

4.1. Evaluation of the active biomass

As proposed by Schaechter et al. (1958), in the model the ratio of cell wall to cell membrane per nucleus remains constant for every growth rate. The active biomass will be represented by X_H, i.e., the mass of structural components built of one nucleus, cell membrane, and cell wall. As the ratio of these structural components is assumed constant, evaluation of active cells as X_H can be performed by measurements of DNA concentration using a COD/DNA ratio.

According to the model assumptions, during exponential growth, the decay of active cells is not significant. Therefore in such experiment, the COD of suspended solids is equivalent to the COD of the cells ($X_H + E_G + B_{STO}$). The concentration of active cells ($X_H + E_G$) will be given by the COD of suspended solids minus that of B_{STO}. Also, the increase in growth rate is linked to an increase of E_G/DNA. The increase of COD per active cells (($X_H + E_G$)/DNA) will give the increase of COD of E_G/DNA. The concentration of active cells ($X_H + E_G$) minus the COD of E_G will give the COD/DNA of X_H. Thus, with a DNA measurement, the X_H concentration expressed as COD should be available.

4.2. Evaluation of kinetic coefficients

Identification of parameters is done most easily by taking advantage of differences in relaxation times, or time constants. According to Roels (1982), the mass action law (substrate saturation) operates within milliseconds, mRNA control in a matter of minutes, enzyme production in a matter of hours, and selection within a population in a matter of days. It is possible to turn these time constants to our advantage and make some simplifications in methods used for parameter evaluation. For instance, it is possible to choose an experimental design for evaluation of a particular coefficient and make the assumption that variables changing with larger time constant have constant value.

It is well known that the saturation of enzymes is reached within a few seconds, and usually this time constant is set to zero. According to the relaxation time as proposed by Roels (1982), in a batch experiment the observable variables will increase or decrease along a sequence as explained below. The first one to increase will be the DNA transcript (Oerther et al. 2002; Cangelosi and Brabant 1997). This first increase of mRNA (mR in the model) induces a rapid increase of the growth rate. After the initial increase, the growth rate and RNA concentration per cell remain constant for at least 2 h (Kjeldgaard et al. 1958). Daigger and Grady (1982*a*) called this first increase of the growth rate "the available reaction potential". The second observable variable is the stable rRNA concentration (E_G in the model), which showed a slow and gradual increase (Cangelosi and Brabant 1997; Muttray et al. 2001; Oerther et al. 2002). This increase of stable rRNA concentration is correlated to the increase of the growth rate (Muttray et al. 2001). According to data presented by Daigger and Grady (1982*a*), this slow increase of the growth rate could take several hours and is preceded by a lag phase. The length of the lag phase is

dependent on the initial growth conditions, i.e., on the induction level of the sludge (the initial ratio E_G/X_H in the model). In the model, as the synthesis rate of E_G is dependent on its own concentration, the duration of this lag phase will be dependent on the initial concentration of E_G. Hence, the model is in agreement with the "unifying theory" proposed by Daigger and Grady (1982*a*).

Also, within biomass grown in a chemostat, by definition, different species of bacteria have the same growth rate. As discussed by Lavallée et al. (2005), selection within a population will take place with the difference between the growth rates of these species. Thus, during the first few hours of a batch culture, the differential growth rate is small, and selection should not occur to a significant level.

Therefore, in a batch experiment, parameters can be identified one at a time on a simple curve fit with adequate measurements. Albertson et al. (1990) observed an increase of the translation rate and a corresponding increase of the respiration after a substrate step-increase in batch experiments. Thus, DNA should be measured to estimate μ_H, and respiration rate for identification of parameters associated with mR and E_G/X_H. As mR has a short half-life, a quick variation of μ_H will be caused by mR dynamics. A slow variation of μ_H will be caused by E_G/X_H variation as it has a greater half-life. As discussed by Lavallée et al. (2005), during exponential growth, the death of active biomass (caused by toxin) is close to zero. Hence, independent identification of the growth rate of X_H and the production rate of E_G and mR is possible.

Obviously, during a batch experiment, release of substrate and storage could influence the growth curve. Hence, if glucose is used as soluble substrate, the glucose concentration and soluble COD concentration will have to be measured. Accordingly, the specific substrate uptake rate can be evaluated. A curve fit will give the uptake enzyme concentration (E_{B_S}/X_H) when the specific rate reaches a constant value. A curve fit on the increase rate of the specific substrate uptake rate will give the production rate of the uptake enzyme (α_{EB_S}). Similar methods can be used for identification of the production rates of other enzymes.

The decay of enzymes can be studied during starvation in a batch experiment. Biomass should be starved for several days. According to the time constants, biomass samples should be taken at constant intervals to build a time series. Consequently, the decline of the growth rate or of the specific activity could be evaluated by performing pulse substrate addition experiments, as done by Vanrolleghem et al. (1998). The half-life of mRNA is in the order of a few minutes, and the half-life of stable rRNA or proteins is a few hours. The decline of the specific respiration rate during starvation should give the decay rate of mR (at the beginning of starvation with an interval of minutes) and of E_G (during the first day of starvation with an interval of hours).

Identification of the decay rate of active biomass should be performed by measurement of the decay rate of the endogenous DNA concentration.

Y_H will be obtained with the usual method for ASM calibration (Henze at al. 2000). As the time constant of the stable rRNA is in the order of hours, one could assume that the variation of rRNA will be limited during short experiments. The heterotrophic yield can thenbe determined from eqs. [13] and [14]. Here, eq. [13] is written two ways, but both expressions have the same meaning. The substrate used should contain only soluble organic matter. If the substrate uptake and storage process occur simultaneously, eq. [13] could be used. At the end of substrate uptake, the yield on stored product could be assessed with eq. [14]. B_S is assumed to be negligible at the beginning and the end of the experiment.

$$Y_{B_S} = \frac{(\Delta \text{ suspended solids COD} - \Delta B_{STO})/Y_H + \Delta B_{STO} + \left(rO_{2\,\text{maintenance}}/Y_H\right)\Delta t}{\Delta \text{ soluble COD}}$$

[13]

$$Y_{B_S} = \frac{\Delta\left[(X_H + E_G)/Y_H\right] + \Delta B_{STO} + \left[(1 - Y_H)/Y_H\right] E_G \beta_{E_G} \Delta t}{\Delta \text{ soluble COD}}$$

After exhaustion of soluble substrate one can evaluate the actual growth yield on B_S.

[14] $$Y_H = \frac{\Delta(E_G + X_H) + (1 - Y_H)\, E_G \beta_{E_G} \Delta t}{\Delta B_{STO}}$$

However, it is assumed that no respiration is associated with the synthesis of storage product ($Y_{B_{STO}/B_S} = 1$). As discussed by Dircks et al. (2001), a gap of only 4% is observed between the yield of biomass on internal substrate and the yield of biomass on storage product. This simplification is required for the easy independent identification of the yield constant Y_{B_S} and Y_H.

The kinetic constants of the hydrolysis process can be identified from a curve fit on data from batch experiments (as carried out by Orhon et al. (1999) and Goel et al. (1998)). With sludge taken from chemostats operated at different dilution rates, the batch experiments will give different initial k_h values for the different sludges. The increase of the k_h rate along the experiment will give the α_{E_h} value. k_h^{max} will be found from a curve

fit on the k_h variation and the corresponding value of E_h.

The variation of the structure of the population remains unknown. However, it is known that selection within a population can take more than days or weeks, and the time constant of this function is large (Roels 1982). Therefore, short experiments can be performed in which the population structure is assumed to be constant. Further research is required to obtain a formulation of this function.

5. Fitting the model to data

The value of a model is often expressed by its capacity to fit data. Therefore, data found in the literature were fitted with the model. It was built on GPS-X™ using the spreadsheet utility Model Developer (Hydromantis Inc., Canada).

Under aerobic conditions, the oxygen uptake rate (OUR) can be associated with the active biomass concentration and its specific activity. Some specific activity fluctuations (or specific growth rate fluctuations) are related to "endogenous variables" such as the mR and E_G levels. This complex behaviour can be observed in the data of Vanrolleghem et al. (1998) for OUR start-up phenomena when sludge starved for 12 h was dosed with three pulses of S_S at 22-min intervals (Fig. 3). The start-up phenomenon could be explained as follows: the growth process induces an increase of the specific activity and starvation induces a loss of specific activity, resulting is a rise and a drop in growth rate and in OUR, respectively (Albertson et al. 1990). Albertson et al. (1990) observed a rapid increase of the transcription rate in the first 60 s. After the first minute, the translation rate increased and within the first 10 min it reached five times the initial rate. This was accompanied by a proportional increase of the respiration rate. This behaviour is similar to that observed by Vanrolleghem et al. (1998). With the model, this behaviour is simulated as follows. Because mR has a short half-life, a decrease of the mR pool occurs during the 12 h starvation period and after the exhaustion of the substrate. The available substrate is used for reconstruction of the mR pool, raising the specific OUR, as shown in the two first substrate pulses in Fig. 4. After the second pulse, the mR concentration reaches the saturation level, and the decline of the specific activity associated with a decay of the mR concentration is not observed on the third pulse. The proposed analysis is a simplified view of time-varying PSS activity, but the fit of the model with this experiment gives good agreement with the data.

With this simple experiment it is possible to identify β_{mR} and also α_{mR}, since the time constant of E_G is larger. Indeed, the fit was quite sensitive to α_{mR} and β_{mR}. No storage occurred as no tailing of OUR was observed. The calculated level of internal substrate was always less than COD of 5 mg/L (of bulk liquid), and this value is in agreement with those observed in the literature (Chassagnole et al. 2002; Vanrolleghem et al. 2004). Moreover, it was not possible to model the observed variation using only substrate uptake and storage without using the dynamics of the variable [mR]. Also, the identified value of β_{mR} gives a half-life of 20 min. This value is of the same magnitude as the half-life of mRNA found in literature (Östling et al. 1993). Thus, the proposed mathematical formulation seems to be in agreement with the real processes. The parameters identified using this experiment are given in Table 4. The parameters identified in the fitting on data of Vanrolleghem et al. (1998) were used to fit other parameters representing slow processes to data first presented by Chiu et al. (1973). In these experiments, bacteria were cultivated in chemostats with imposed dilution rates, and the cells were taken out of the chemostats and put in batch reactors. Daigger and Grady (1982*a*) re-examined these data and showed that an increase of growth rate took place within a few hours after the shift up and that the lag phase was dependent on the initial growth conditions.To perform the fit shown on Fig. 5, only the initial values of state variables as X_H, E_G, [mR], $E_{B_{S(1)}}$ and $E_{B_{S(2)}}$ were changed. The set of parameters used is given in Table 5. The parameters related to the uptake processes (in r2 and r8) were identified using the substrate concentration data from Chiu et al.'s batch experiments (data not showed). To minimize the number of degrees of freedom, only the substrate uptake and the growth and storage processes were modeled. The other processes (r9 to r13, and r20 to r25) were set to zero. Additional data are required to identify the parameters included in these processes. In the fit of Vanrolleghem et al.'s (1998) data, shown in Fig. 4, the $K_{S(1)} = 0.2$ mg/L was used. To perform the fit of Chiu et al.'s data, the $K_{S(2)}$ value was set close to 40 mg/L. These different values are of the same magnitude as those obtained by Chiu et al. (1973) in steady-state culture with dilution rates of 0.022 and 0.6 h^{-1}, respectively, or by Ferenci (1999) for two transport enzymes. The batch experiment favours the induction of an uptake system with low affinity and high capacity and therefore increases the specific substrate uptake rate and the observed K_S value, as seen in these fits. The observed K_S value and the specific substrate uptake rate change according to the relative induction of the two transport systems. The values of β_{E_A} and enzyme decay (β_{E_X}) were chosen according to literature values (Aizenman et al. 1996; Cozzone 1981). Finally, all the data shown were fitted with the single set of parameters identified. Thus, with the same set of parameters, the model is able to describe short and long transients. It is not possible to fit all these data with the usual ASM without changing the values of the parameters because $\mu_{H\,max}$

Fig. 4. OUR start-up phenomenon observed when 3 pulses of S_S are dosed (data from Vanrolleghem et al. 1998).

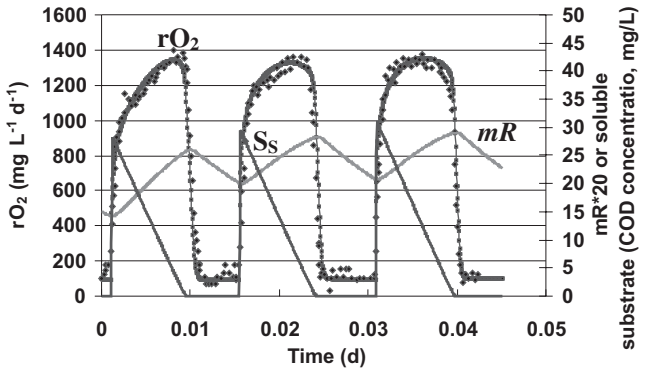

Table 4. Identified parameters on experiment of Vanrolleghem et al. (1998).

Parameter	Symbol	Units	Value
Maximal heterotrophic growth rate	μ_H	d^{-1}	30
Yield coefficient	Y_{B_S}	COD/COD, g/g	0.92
Half saturation constant	$K_{S(1)}$	COD, mg/L	0.2
Half saturation constant	K_{B_S}	mg mg^{-1}	0.0015
Half saturation constant	K_{mR}	unit mg^{-1}	0.007
Ratio of production rate of E_G and μ_H	φ_{E_G}	mg mg^{-1}	1.3
Production rate of mR	α_{mR}	d^{-1}	0.75
Production rate of $E_{BS(1)}$	$\alpha_{E_{BS(1)}}$	d^{-1}	15
Maximum specific activity of substrate uptake enzyme (1)	$k^{max}_{B_{S(1)}}$	COD, g g^{-1} d^{-1}	41
Decay rate of mR	β_{mR}	h^{-1}	2.083

Table 5. Additional parameters used to perform the fits of Chiu et al. (1973).

Parameter	Symbol	Units	Value
Yield coefficient	Y_H	COD/COD, g/g	0.73
Half saturation constant	$K_{S(2)}$	COD, mg/L	40
Maximum specific activity of substrate uptake enzyme (1)	$k^{max}_{B_{S(1)}}$	COD, g g^{-1} d^{-1}	10
Maximum specific activity of substrate uptake enzyme (2)	$k^{max}_{B_{S(2)}}$	COD, g g^{-1} d^{-1}	26
Maximum specific activity of storage enzyme	k^{max}_{STO}	COD, g g^{-1} d^{-1}	8
Maximum specific activity of degradation enzyme of storage product	δk^{max}_{STO}	COD, g g^{-1} d^{-1}	5
Half saturation constant	K_{STO}	(COD of B_{STO})/(COD of X_H), mg mg^{-1}	0.7
Production rate of $E_{B_{S(2)}}$	$\alpha_{E_{B_{S(2)}}}$	d^{-1}	51
Production rate of E_{STO}	$\alpha_{E_{STO}}$	d^{-1}	43
Decay rate of E_G	β_{E_G}	d^{-1}	1.44
Decay rate of $E_{B_{S(1)}}$	$\beta_{E_{B_{S(1)}}}$	d^{-1}	1.44
Decay rate of $E_{B_{S(2)}}$	$\beta_{E_{B_{S(2)}}}$	d^{-1}	1.44
Decay rate of E_{STO}	$\beta_{E_{STO}}$	d^{-1}	1.44

Fig. 5. Fit of lag phase (data from Chiu et al. 1973).

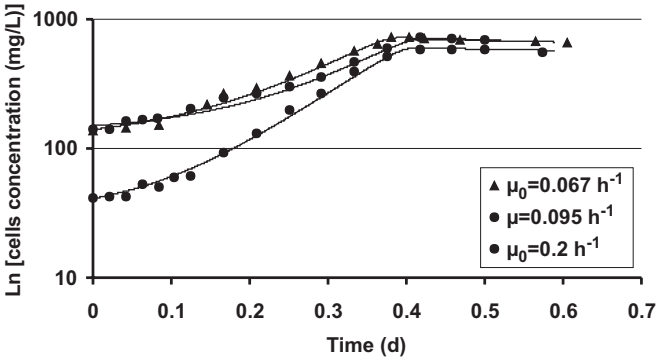

Fig. 6. Fit of a lag phase (data from Chiu et al. 1973).

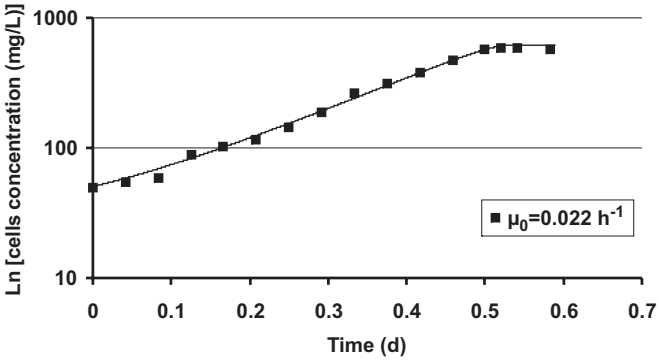

varies during these experiments. With Chiu et al.'s (1973) data, ASMs will simply give straight lines with the same slope. With Vanrolleghem et al.'s (1998) data, ASM1 will give three square waves and ASM3 will give three identical waves with tailing.

To model the data presented in Fig. 6, the yield value (Y_H) used to perform the fit was lower ($Y_H = 0.66$) than the one used for modeling of the other experiments ($Y_H = 0.73$). In Fig. 6, one sees that the initial growth rate was 0.022 h^{-1}, lower than those in Fig. 5. The lower yield might be justified by an uncoupling between the growth process and the oxidation process under a critical growth rate (Daigger and Grady 1982*b*). The uncoupling phenomenon is not modeled here. Hence, it was necessary to modify the yield coefficient to perform the fit with a low initial growth rate. To perform the fit with a Y_H of 0.73 (Fig. 6), some trials were done using several values of E_G turnover; however, a higher turnover of this component had a significant impact on the growth process but only a small one on the observed yield. Alternatively, an increase in soluble microbial product production was modeled with the B_S release process. This process had a significant impact on the substrate concentration but still only a small one on the observed yield. This deficiency in the description of the biomass is a limit in

Fig. 7. Simulated variation of cell characteristics during a batch experiment ($\mu_0 = 0.095\ h^{-1}$).

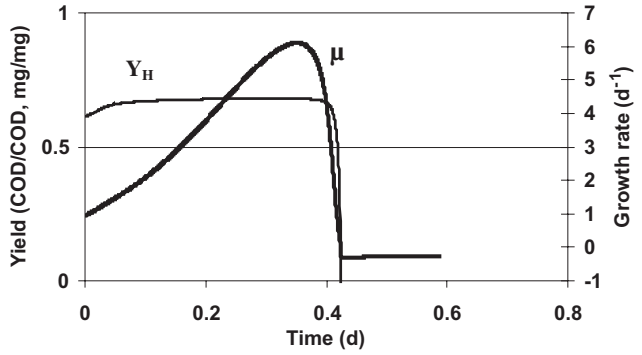

Fig. 8. Simulated relative concentrations of components during a batch experiment ($\mu_0 = 0.095\ h^{-1}$).

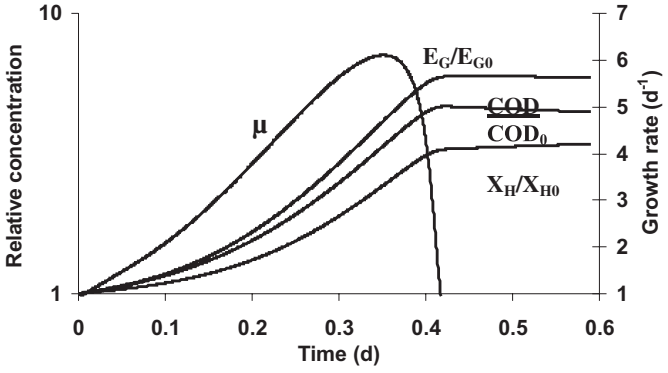

the application of the model. Perhaps futile cycles should be included in the model to enlarge the application range of the model.

Nevertheless, the turnover of E_G had some impact on the yield. Figure 7 shows the typical variation of the yield during the batch experiment. In the first phase of the experiment, the growth rate is low, and the maintenance of E_G uses a greater fraction of the substrate taken up. As the growth rate increases, the percentage of substrate used for the maintenance process decreases and the yield increases. Thus, in steady-state culture, the maintenance process decreases the observed yield, as discussed by Pirt (1965). Also, although the death of active cells was set to zero, after the substrate exhaustion the growth rate is negative, as discussed by Herbert (1958). For a starving biomass, the turnover of E_G ($\beta_{E_G} = 0.06\ h^{-1}$) gave a respiration close to that of the usually observed endogenous respiration (2 to 5mg of O_2 per hour per gram of volatile suspended solids) of activated sludge or that calculated with the decay rate default value in ASM (Avcioglu et al. 1998; Henze et al. 2000; Lavallée et al. 2002).

The relative concentrations of E_G and X_H and the growth rate are shown in Fig. 8. The cell components are expressed as a ratio to the initial concentration. In this figure one can see that between 0 and 0.17 d, the growth rate increases faster than the E_G component, indicating that the [mR] variable has an influence on the growth rate. Between 0.17 and 0.27 d the growth rate increases at the same rate as E_G, indicating that E_G is rate limiting according to the RNA-limiting theory (Daigger and Grady 1982*b*). After 0.27 d the growth rate increases slower than E_G, indicating that another process has become rate-limiting. The exogenous substrate concentration becomes rate-limiting ($S_S < 2K_{S(2)}$) only after 0.37 d, and according to the calibration procedure, in such circumstances the substrate uptake is rate limiting. This analysis is in agreement with the analysis done by Daigger and Grady (1982*b*) on RNA, proteins, and DNA production rates in similar experiments. Hence, the use of the proposed model could help in the understanding of transients behaviours occurring in activated sludge under organic shock loads, for instance. Obviously this should be done with care, and several validation steps of the model on appropriate data remain to be performed.

6. Conclusion

The proposed model gives a more realistic picture of active biomass and of its specific activity, but further research is required to support the model with experimental data. This model allows fitting of several data sets found in the literature with a single set of parameters. It therefore improves the quality of the kinetic information obtained by parameter estimation. Also, through the use of DNA measurement to estimate active biomass, it will be possible to assess the specific values of parameters. This will help to increase our understanding of processes occurring within cells under transients. If the specific activity description of biomass gives a good description of the real behaviour of the active biomass under transient, the proposed formulation will make the kinetic constant evaluation a procedure that is independent of sludge age and of the process configuration. Thus, after substrate characterization, a single set of values for kinetic parameters would fit the response of different processes. This will eventually make the model a helpful tool for research and understanding of treatment processes.

The formulation of the proposed model opens several topics of further research. Thus, considerable work is still to be done to explore these new areas. Several validation steps of the model on appropriate data remain to be performed.

Acknowledgements

The Natural Sciences and Engineering Council of Canada and the Fond Québécois pour la Formation de Chercheurs et l'Aide la Recherche are acknowledged for their financial support. Also, part of this work was financially supported by the Fund for Scientific Research – Flanders (FWO-Vlaanderen), project G.0184.04.

References

Aizenman, E., Engelberg-Kulka, H., and Glaser, G. 1996. An *Escherichia coli* chromosomal "addiction module" regulated by

guanosine 3', 5'-bispyrophosphate: a model for programmed bacterial cell death. Proc. Natl. Acad. Sci. U.S.A. **93**: 6059–6063.

Albertson, N.H., Nyström, T., and Kjelleberg, S. 1990. Macromolecular synthesis during recovery of the marine *Vibrio* sp. S14 from starvation. J. Gen. Microbiol. **136**: 2201–2207.

Avcioglu, E., Orhon, D., and Sözen, S. 1998. A new method for the assessment of heterotrophic endogenous respiration rate under aerobic and anoxic conditions. Water Sci. Technol. **38**(8–9): 95–103.

Bailey, J.E., and Ollis, D.F. 1986. Biochemical engineering fundamentals. 2nd ed. McGraw-Hill Book Company, New York.

Baloo, S., and Ramkrishna, D. 1991. Metabolic regulation in bacterial continuous cultures: 1. Biotechnol. Bioeng. **38**: 1337–1352.

Beeftink, H.H., van der Heijden, R.T.J.M., and Heijnen, J.J. 1990. Maintenance requirements: energy supply from simultaneous endogenous respiration and substrate consumption. FEMS Microbiol. Ecol. **73**: 203–210.

Berlyn, M.K.B., Low, K.B., and Rudd, K.E. 1996. Linkage map of *Escherichia coli* K-12, Edition 9. *In Escherichia coli* and *Salmonella*, cellular and molecular biology. Vol. 2. *Edited by* F.C. Neidhardt, R. Curtiss, J.L. Ingraham, E.C.C. Lin, K.B. Low, B. Magasanik, W.S. Reznikoff, M. Riley, M. Schaechter, and H.E. Umbarger. ASM Press, Washington, D.C. pp. 1715–1805.

Beun, J.J., Paletta, F., van Loosdrecht, M.C.M., and Heijnen, J.J. 2000. Stoichiometry of poly-β-hydroxybutyrate metabolism in aerobic, slow growing, activated sludge cultures. Biotechnol. Bioeng. **67**: 379–389.

Brands, E., Liebeskind, M., and Dohmann, M. 1994. Parameters for dynamic simulation of wastewater treatment plants with high-rate and low-rate activated sludge tanks. Water Sci. Technol. **30**(4): 211–214.

Bremer, H., and Dennis, P.P. 1996. Modulation of chemical composition and other parameters of the cell by growth rate. *In Escherichia coli* and *Salmonella*, cellular and molecular biology. Vol. 2. *Edited by* F.C. Neidhardt, R. Curtiss, J.L. Ingraham, E.C.C. Lin, K.B. Low, B. Magasanik, W.S. Reznikoff, M. Riley, M. Schaechter, and H.E. Umbarger. ASM Press, Washington, D.C. pp. 1553–1569.

Cangelosi, G.A., and Brabant, W.H. 1997. Depletion of pre-16S rRNA in starved *Escherichia coli* cells. J. Bacteriol. **179**(14): 4457–4463.

Chassagnole, C., Noisommit-Rizzi, N., Schmid, J.W., Mauch, K., and Reuss, M. 2002. Dynamic modeling of the central carbon metabolism of *Escherichia coli*. Biotechnol. Bioeng. **79**: 53–73.

Chiu, S.Y., Kao, I.C., Erickson, L.E., and Fan, L.T. 1973. ATP pool in activated sludge. J. Water Pollut. Control Fed. **45**(8): 1746–1758.

Chudoba, P., Capdeville, B., and Chudoba, J. 1992. Explanation of biological meaning of the S_0/X_0 ratio in batch cultivation. Water Sci. Technol. **26**(3–4): 743–751.

Çinar, Ö., and Grady, C.P.L., Jr. 2001. Aerobic and anoxic biodegradation of benzoate: stability of biodegradative capability under endogenous conditions. Water Res. **35**(4): 1015–1021.

Cozzone, A.J. 1981. How do bacteria synthesize proteins during amino acid starvation? Trends Biochem. Sci. **6**(4): 108–110.

Daigger, G.T., and Grady, C.L.P., Jr. 1982*a*. The dynamics of microbial growth on soluble substrate A unifying theory. Water Res. **16**: 365–382.

Daigger, G.T., and Grady, C.L.P., Jr. 1982*b*. An assessment of the role of physiological adaptation in the transient response of bacterial cultures. Biotechnol. Bioeng. **24**: 1427–1444.

Dircks, K., Beun, J.J., van Loosdrecht, M., Heijnen, J.J., and Henze, M. 2001. Glycogen metabolism in aerobic mixed cultures. Biotechnol. Bioeng. **73**(2): 85–94.

Ferenci, T. 1999. 'Growth of bacterial cultures' 50 years on: towards an uncertainty principle instead of constants in bacterial growth kinetics. Res. Microbiol. **150**: 431–438.

Frigon, D., Oerther, D.B., Morgenroth, E., and Raskin, L. 2002*a*. Oligonucleotide probe hybridization and modeling results suggest that populations consuming readily degradable substrate have high cellular RNA levels. Water Sci. Technol. **45**(6): 115–126.

Frigon, D., Arnaiz, E., Oerther, D.B., and Raskin, L. 2002*b*. Who eats what? Classifiing microbial population based on diurnal profiles of rRNA levels. Water Sci. Technol. **46**(1–2): 1–9.

Goel, R., Takashi, M., Hiroyasu, S., and Matsuo, T. 1998. Comparison of hydrolytic enzyme system in pure culture and activated sludge under different electron acceptor conditions. Water Sci. Technol. **37**(4–5): 335–343.

Grady, C.L.P., Harlow, L.J., and Riesing, R.R. 1972. Effects of growth rate and influent substrate concentration on effluent quality from chemostats containing bacteria in pure and mixed culture. Biotechnol. Bioeng. **14**: 391–410.

Grady, C.P.L., Jr., Smets, B.F., and Barbeau, D.S. 1996. Variability in kinetic parameter estimates: a review of possible causes and a proposed terminology. Water Res. **30**(3): 742–748.

Haider, S., Vanrolleghem, P.A., and Kroiß, H. 2000. Low sludge age and its consequences for metabolisation, storage and adsorption of readily biodegradable substrate (Ss). *In* Proceedings of the 1st World Congress of the International Water Association. Paris, France, 3–7 July 2000. [CD-ROM].

Hanada, S., Hiroyasu, S., and Mino, T. 2001. Measurement of microorganisms with PHA production capability in activated sludge and its implication in activated sludge model no. 3. Water Sci. Technol. **45**(6): 107–113.

Hao, O.J., and Lau, A.O. 1988. Kinetics of microbial by-product formation in chemostat pure cultures, ASCE J. Environ. Eng. **114**(5): 1097–1115.

Henze, M., Gujer, W., Mino, T., and van Loosdrecht, M. 2000. Activated sludge models ASM1, ASM2, ASM2d and ASM3. IWA Publishing, London, U.K.

Herbert, D. 1958. Some principles of continuous culture. *In* Recent progress in microbiology. *Edited by* G. Tunevall. 7th International Congress for Microbiology, Stockholm, Sweden, 4–9 August 1958. pp. 381–396.

Herbert, D. 1976. Stoichiometric aspects of microbial growth. *In* Continuous culture 6: applications and new field. *Edited by* A.C.R. Dean, D.C. Ellwood, C.G.T. Evans, and J. Melling. Elis Horwood Ltd., Chichester, U.K. pp. 1–30.

Huang, J.Y.C., and Cheng, M.D. 1987. Transient responses incorporating products formation. ASCE J. Environ. Eng. **113**(4): 868–880.

Jensen, K.F., and Pedersen, S. 1990. Metabolic growth rate control in *Escherichia coli* may be a consequence of subsaturation of the macromolecular biosynthetic apparatus with substrates and catalytic components. Microbiol. Rev. **54**(2): 89–100.

Kjeldgaard, N.O., Maaloe, O., and Schaechter, M. 1958. The transition between different physiological states during balanced growth of *Salmonella typhimurium*. J. Gen. Microbiol. **19**: 607–616.

Kompala, D.S., Ramkrishna, D., Jansen, N.B., and Tsao, G.T. 1986. Investigation of bacterial growth on mixed substrates: experimental evaluation of cybernetic models. Biotechnol. Bioeng. **28**: 1044–1055.

Kovárová-Kovar, K., and Egli, T. 1998. Growth kinetics of suspended microbial cells: from single-substrate-controlled growth to mixed-substrate kinetics. Microbiol. Mol. Biol. Rev. **62**(3): 646–666.

Lavallée, B., Lessard, P., and Besser, C. 2002. Decay rate variability of heterotrophic active biomass. Water Sci. Technol. **46**(1–2): 423–430.

Lavallée, B., Lessard, P., and Vanrolleghem, P.A. 2005. Review of prokaryote metabolism in view of modeling of activated sludge adaptation to multiple process configuration. J. Environ. Eng. Sci. In press.

Lee, D.-U., Casasús-Zambrana, A., Hamilton, R., Svoronovos, S., Lee, S.-I., and Koopman, B. 2004. Significance of denitrifying enzyme dynamics in biological nitrogen removal processes: a simulation study. Water Sci. Technol. **49**(5–6): 265–274.

Liu, P.-H., Zhan, G., Svoronos, S.A., and Koopman, B. 1998. Diauxic lag from changing electron acceptors in activated sludge treatment. Water Res. **32**(11): 3452–3460.

Masson, C.A., Hamer, G., and Bryers, J.D. 1986. The death and lysis of micro-organisms in environmental processes. FEMS Microbiol. Rev. **39**: 373–401.

Monod, J. 1949. The growth of bacterial cultures. Annu. Rev. Microbiol. **3**: 371–394.

Muttray, A.F., Yu, Z., and Mohn, W.W. 2001. Population dynamics and metabolic activity of *Pseudomonas abietaniphila* BKME-9 within pulp mill wastewater microbial communities assayed by competitive PCR and RT-PCR. FEMS Microbiol. Ecol. **38**: 21–31.

Nicolaï, B.M., Van Impe, J.F., Vanrolleghem, P.A., and Vandewalle, J. 1991. A modified unstructured mathematical model for the penicillin G fed-batch fermentation. Biotechnol. Lett. **13**: 489–494.

Oerther, D.B., van Loosdrecht, M.C.M., and Raskin, L. 2002. Quantifying the impact of wastewater micronutrient composition on in situ growth activity of *Acinetobacter* spp. Water Sci. Technol. **46**(1–2): 443–447.

Orhon, D., Çokgör, U.E., and Sözen, S. 1999. Experimental basis for the hydrolysis of slowly biodegradable substrate in different wastewaters. Water Sci. Technol. **39**(1): 87–95.

Östling, J., Holmquist, L., Flärdh, K., Svenblad, B., Jouper-Jaan, A., and Kjelleberg, S. 1993. Starvation and recovery of *Vibrio*. *In* Starvation in bacteria. *Edited by* S. Kjelleberg. Plenium Press, New York, London. pp. 103–127.

Pirt, S.J. 1965. The maintenance energy of bacteria in growing cultures. Proc. R. Soc. London, Ser. B, **163**: 224–231.

Priest, F.G. 1992. Synthesis and secretion of extracellular enzymes in bacteria. *In* Microbial degradation of natural products. *Edited by* G. Winkelman. VCH Publisher, Inc., New York. pp. 1–27.

Ramkrishna, D. 1983. A cybernetic perspective of microbial-growth. *In* Foundations of biochemical engineering — kinetics and thermodynamics in biological systems. *Edited by* H.W. Blanch, E.T. Papoustakis, and G. Stephanopoulos. ACS Symposium Ser. 207, American Chemical Society, Washington, D.C. pp. 161–178.

Reichert, P., Borchardt, D., Henze, M., Rauch, W., Shanahan, P., Somlyody, L., and Vanrolleghem, P.A. 2001. River Water Quality Model No. 1, Scientific & Technical Report No. 12. IWA Publishing, London, U.K.

Roels, J.P. 1982. Mathematical models and the design of biochemical reactors. J. Chem. Biotechnol. **32**: 59–72.

Schaechter, M., Maaloe, O., and Kjeldgaard, N.O. 1958. Dependency on medium and temperature of cell size and chemical composition during balanced growth of *Salmonella typhimurium*. J. Gen. Microbiol. **19**: 592–606.

Sin, G. 2004. Systematic calibration of activated sludge models. Ph.D. thesis, Ghent University, Ghent, Belgium.

Turner, B.G., Ramkrishna, D., and Jansen, N.B. 1989. Cybernetic modeling of bacterial cultures at low growth rates: single-substrate systems. Biotechnol. Bioeng. **34**: 252–261.

van den berg, H.A. 1998. A generic view of classic microbial growth models. Acta Biotheor. **46**: 117–130.

van Loosdrecht, M.C.M., and Henze, M. 1999. Maintenance, endogenous respiration, lysis, decay and predation. Water Sci. Technol. **39**(1): 107–117.

van Loosdrecht, M.C.M., Pot, M.A., and Heijnen, J.J. 1997. Importance of bacterial storage polymers in bioprocesses. Water Sci. Technol. **35**(1): 41–47.

Vanrolleghem, P.A., Gernaey, K., Petersen, B., De Clercq, B., Coen, F., and Ottoy, J.-P. 1998. Limitations of short-term experiments designed for identification of activated sludge biodegradation models by fast dynamic phenomena. *In* Proceedings of the 7th IFAC Conference on Computer Applications in Biotechnology CAB7, Osaka, Japan, 31 May–4 June 1998. pp. 567–572.

Vanrolleghem, P.A., Sin, G., and Gernaey, K. 2004. Transient response of aerobic and anoxic activated sludge activities to sudden substrate concentration changes. Biotechnol. Bioeng. **86**(3): 277–290.

Yarmolinsky, M.B. 1995. Programmed cell death in bacterial populations. Science, **267**: 836–837.

Zhang, X., Dennis, P., Ehrenberg, M., and Bremer, H. 2002. Kinetic properties of *rrn* promoters in *Escheriachia coli*. Biochimie, **84**: 981–996.

List of symbols

b_{MF}	death rate coefficient of micro fauna (d^{-1})
$b_{X_T}^{max}$	maximum death rate coefficient of biomass related to toxin X_T (d^{-1})
B_S	concentration of endogenous substrate B_S (COD, mg L^{-1})
B_{STO}	concentration of stored endogenous substrate B_{STO} (COD, mg L^{-1})
E_A	concentration of antitoxin enzyme E_A (unit L^{-1})
E_{B_S}	concentration of transport enzyme E_{B_S} (unit L^{-1})
E_G	concentration of growth enzyme E_G (unit L^{-1})
E_h	concentration of hydrolysis enzyme E_h (unit L^{-1})
E_{STO}	concentration of storage enzyme E_{STO} (unit L^{-1})
E_T	concentration of toxin enzyme E_T (unit L^{-1})
f_u	non-biodegradable fraction of particulate material (COD, mg mg^{-1})
i_{XB}	nitrogen fraction of active biomass (X_H) and growth enzyme (E_G) (mg N per (mg COD))
$k_{B_S}^{max}$	maximum specific activity of uptake enzyme E_{B_S} (d^{-1})
k_h	specific activity of hydrolysis enzyme (E_h) (d^{-1})
k_h^{max}	maximum specific activity of hydrolysis enzyme (E_h) (d^{-1})
$k_{RB_S}^{max}$	maximum release rate of endogenous substrate B_S (d^{-1})
k_{STO}^{max}	maximum specific activity of storage process enzyme E_{STO} (d^{-1})
K_{B_S}	affinity constant for endogenous substrate (COD, mg mg^{-1})
K_{iT}	half saturation coefficient of toxin inhibition for the antitoxin (unit mg^{-1})
K_{MFO}	affinity constant of microfauna for dissolved oxygen (O_2, mg L^{-1})

K_{mR} affinity constant for mR (unit mg^{-1})
K_{NH} affinity constant for ammonia (N, mg L^{-1})
K_O affinity constant for dissolved oxygen (O_2, mg L^{-1})
K_{RB_S} affinity constant of substrate release process for endogenous substrate (COD, mg mg^{-1})
$K_{S(1or2)}$ affinity constant of transport process 1 or 2 for soluble substrate (COD, mg L^{-1})
K_{STO} affinity constant for stored product (mg COD per (mg COD of X_H))
$K_{X/MF}$ affinity constant of growth of protozoa for biomass (COD, mg L^{-1})
K_{X_S} affinity constant for particulate substrate (COD, mg L^{-1})
[mR] concentration of mR, the short half life component of the PSS (unit L^{-1})
$r_{O_2\ \text{maintenance}}$ respiration rate related to maintenance (O_2 mg L^{-1} d^{-1})
S_0 initial concentration of substrate (COD, mg L^{-1})
S_{NH} concentration of ammonia (N, mg L^{-1})
S_O concentration of dissolved oxygen (O_2, mg L^{-1})
S_S concentration of soluble substrate (COD, mg L^{-1})
X_0 initial concentration of biomass (COD, mg L^{-1})
X_H concentration of heterotrophic organisms (COD, mg L^{-1})
X_{MF} concentration of microfauna, including protozoa and metazoa (COD, mg L^{-1})
Y_{B_S} yield coefficient of endogenous substrate on exogenous substrate (mg COD of B_S per (mg COD of S_S))
Y_{B_{STO}/B_S} yield coefficient of storage product on endogenous substrate (mg COD of B_{STO} per (mg COD of B_S))
Y_H yield coefficient of biomass on stored product (mg COD of cell per (mg COD of B_{STO}))
Y_{MF} yield coefficient of microfauna on bacteria (mg COD of protozoa per (mg COD of X_H))
α_{EA} production rate of antitoxin enzyme E_A (d^{-1})
$\alpha_{E_{BS(1or2)}}$ production rate of uptake enzyme $E_{B_{S(1or2)}}$ (d^{-1})
α_{Eh} inductive production rate of hydrolysis enzyme E_h(d^{-1})
$\alpha_{E_{STO}}$ production rate of storage enzyme E_{STO} (d^{-1})
α_{ET} production rate of toxin enzyme E_T (d^{-1})
α_{mR} production rate of mR (d^{-1})
β_{EA} decay rate of antitoxin enzyme E_A (d^{-1})
$\beta_{E_{BS}}$ decay rate of of uptake enzyme $E_{B_{S(1or2)}}$ (d^{-1})
β_{E_G} decay rate of growth enzyme E_G (d^{-1})
β_{E_h} decay rate of hydrolysis enzyme E_h (d^{-1})
$\beta_{E_{STO}}$ decay rate of transportation enzyme E_{STO} (d^{-1})
β_{E_T} decay rate of toxin enzyme E_T (d^{-1})
β_{mR} decay rate of mR (d^{-1})
δk_{STO}^{max} maximal specific activity of degradation enzyme of storage product (d^{-1})
μ_H growth rate of heterotrophic organisms (d^{-1})
$\mu_{H\,max}^{int}[d^{-1}]$ intrinsic maximum value of growth rate of biomass (d^{-1})
$\mu_{MF\,max}[d^{-1}]$ the maximum growth rate of micro fauna (d^{-1})
φ_{E_G} ratio of production rate of growth enzyme E_G and growth rate (mg/mg)